SCIENCE CHINA
Chemistry

• ARTICLES •

November 2014 Vol.57 No.11: 1552–1558
doi: 10.1007/s11426-014-5145-4

Carbon-free $Cu_2ZnSn(S,Se)_4$ film prepared via a non-hydrazine route

ZOU YuGang, LIU Jie, ZHANG Xing, JIANG Yan, HU JinSong* & WAN Li-Jun*

Beijing National Laboratory for Molecular Sciences; CAS Key Laboratory of Molecular Nanostructure and Nanotechnology; Institute of Chemistry, Chinese Academy of Sciences, Beijing 100190, China

Received April 3, 2014; accepted April 30, 2014; published online September 22, 2014

The kesterite $Cu_2ZnSn(S,Se)_4$ (CZTSSe) is an ideal candidate for light harvesting materials in earth-abundant low-cost thin-film solar cells (TFSC). Although the solution-based processing is a most promising approach to achieve low-cost solar cells with high power conversion efficiency, the issues of poor crystallinity and carbon residue in CZTSSe thin films are still challenging. Herein, a non-hydrazine solution-based method was reported to fabricate highly crystallized and carbon-free kesterite CZTSSe thin films. Interestingly, it was found that the synthetic atmosphere of metal organic precursors have a dramatic impact on the morphology and crystallinity of CZTSSe films. By optimizing the processing parameters, we were able to obtain a kesterite CZTSSe film composed of compact large crystal grains with trace carbon residues. Also, a viable reactive ion etching (RIE) processing with optimized etching conditions was then developed to successfully eliminate trace carbon residues on the surface of the CZTSSe film.

CZTS, CZTSSe, solar cells, carbon, non-hydrazine

1 Introduction

Thin-film chalcogenide photovoltaic (PV) technologies are expected to dominate the next generation solar cell market because of its high performance and possibility of large-area module production [1–4]. With high optical absorption coefficients and appropriate band gaps, CdTe and $Cu(In,Ga)(S,Se)_2$ (CIGSSe) solar cells have achieved a power conversion efficiency (PCE) as high as 19.6% and 20.8%, respectively [5, 6]. However, their practical applications have been limited by either the heavy metal usage for cadmium or the limited supply of tellurium, indium and gallium. To deal with the energy demand in the terawatt scale and environmental concerns in future, the development of solar cell techniques based on low-cost solution processing and earth-abundant materials has attracted much attention and been considered as a prospective direction in tackling future energy crisis [7–9]. Recently, $Cu_2ZnSn(S,Se)_4$ (CZTSSe) in which earth-abundant zinc and tin replace rare metals of indium and gallium in CIGSSe has emerged as a potential substitute for CIGSSe because of its elemental abundance, proper and tunable band gap between 1.0 and 1.5 eV, and high absorption coefficient of 10^5 cm^{-1} [3, 10–18].

The first reported CZTS solar cell with a PCE of 0.66% was fabricated via a vacuum-deposition method in 1996 [16]. For decades, a wide range of vacuum-based approaches have been applied to prepare high-quality CZTSSe thin films [7, 9]. Co-sputtering and co-evaporation are the two most successful techniques among them. By optimizing the deposition conditions and annealing parameters, 9.3% of PCE has been achieved in the co-evaporation route and 9.15% in the co-sputtering route [19, 20]. Apart from the traditional vacuum-deposition methods, researchers have developed several non-vacuum approaches taking into consideration lower cost and higher output [2, 7, 9, 19, 21–25]. Deligianni's group [21] reported 7.3% device efficiency

*Corresponding authors (email: hujs@iccas.ac.cn; wanlijun@iccas.ac.cn)

using an electro-deposition approach. Mitzi's group [10] at the IBM T.J. Watson Research Center developed a new hydrazine-based solution process for fabricating a CZTSSe thin film and achieved a device PCE of 9.66% by spinning a slurry comprised of copper tin chalcogenide solution in hydrazine and dispersible particle-based Zn-chalcogenide precursors ($ZnSe(N_2H_4)$). This work stimulated a growing research in solution processed CZTSSe solar cells. Yang's group [24] also reported a device PCE of 8.1% using a homogeneous hydrazine-based CZTS precursor solution. Recently, Mitzi's group [2] improved their hydrazine-based hybrid particle slurries process and pushed forward the efficiency to 11.1%.

Despite the high conversion efficiency being achieved via the hydrazine-based route, the usage of extremely toxic and explosive hydrazine will undoubtedly restrict the actual application of this method. To avert this issue, it is necessary to develop a safe and non-toxic solvent process. PCE between 6.03% and 8.5% have been reported by several groups using the non-hydrazine solvent system to fabricate the CZTSSe film [25–28]. Unfortunately, all of those reported organic solvents inevitably introduced carbon contamination in the final CZTSSe absorber film [23, 25, 26], which commonly raised the series resistance and became carrier recombination centers, resulting in the decrease in PCE [23, 25, 26, 29]. Because carbon residue in the previous reports was usually underneath the absorber layer or embedded in the layer, it is difficult to get rid of it [11, 27]. Herein we reported a non-hydrazine route to prepare the kesterite CZTSSe absorber film with good crystallinity. It was interestingly found that the ambience during the preparation of the precursor significantly influenced the morphology and crystallinity of the absorber film. By optimizing the processing parameters, we were able to minimize the formation of the carbon residue and move it to the top of the film, followed by the successful removal via reactive ion etching (RIE).

2 Experimental

2.1 General experimental information

CuCl (99.995%, Sigma Aldrich, MO, USA); $ZnCl_2$ (99.99%, Sigma Aldrich, MO, USA); $SnCl_4$ (99.99%, Alfa Aesar, MA, USA); Selenium pill (99.999%, Alfa Aesar, MA, USA); 1-butylamine (99%, Alfa Aesar, MA, USA); ethanol and CS_2 (AR grade, Sinopharm Chemical Reagent Co., Ltd, Shanghai, China). All these commercially available chemicals were used as received.

Mo-coated glass substrates were prepared by sputtering Mo on soda lime glass substrates on a magnetron sputtering system (PVD75, Kurt J. Lesker). The square resistance was 118 mΩ/sq and the thickness of the Mo layer was 1 μm. The morphologies of all CZTSSe films were characterized by scanning electron microscopy (JSM 6701, JEOL, Japan). X-ray diffraction (XRD) experiments were carried out on a Regaku D/Max-2500 diffractometer equipped with a Cu $K\alpha_1$ radiation (λ = 1.54056 Å, Rigaku Corporation, Japan). The Raman spectra were recorded with a DXR SmartRaman Spectrometer from Thermo Fisher Scientific (USA) with a laser wavelength of 532 nm.

2.2 Synthesis of metal organic precursor

In a typical synthesis, CuCl (0.1633 g, 1.65 mmol) and $ZnCl_2$ (0.1400 g, 1.03 mmol) were dissolved in 3 mL ethanol in a 25-mL three-necked flask under an argon flow of 1 mL/min. 6 mL 1-butylamine and 4 mL CS_2 were added after 5 min under stirring. Another 5 min later, 95 μL (0.81 mmol) of anhydrous tin tetrachloride was injected into the flask to get a buff solution. After stirring for 20 min under an argon flow of 0.4 sccm, the mixture was centrifuged at 10000 r/min for 15 min to separate any insoluble components. The clear and yellow supernatant layer was then collected into a serum bottle as a metal organic precursor S1 for the film preparation.

Another precursor solution was prepared for comparison in exactly the same procedure as the synthesis of precursor S1, except for no argon protection. A clear and light red solution was formed and marked as the precursor S2.

2.3 Preparation of CZTS film

CZTS thin films were first prepared by spin-coating the pre-prepared precursor solutions on Mo-coated glass substrates at 2600 r/min for 5 min, followed by the annealing on a hot plate at 340 °C for 3 min. The above procedure was repeated 7 times to achieve a 1.0–1.2 μm thick CZTS thin film. All these procedures were conducted in a N_2 glove box with water and oxygen content below 1 ppm. The films prepared with precursors S1 and S2 were named after CZTS film S1 and S2, respectively.

2.4 Preparation of CZTSSe film

The CZTSSe thin films were obtained by selenizing the prepared CZTS thin films. The as-synthesized CZTS films were placed inside a 15 mm × 150 mm glass tube with a 50 mg selenium pill. The tube was then sealed under vacuum using hydroxide flame. The selenization was conducted under 520 °C for 30 min.

2.5 Reactive ion etching

An inductively coupled reactive ion etching system (ICP-RIE SI500, Sentech Instruments Ltd., Germany) was used to remove the carbon residue on the top of the CZTSSe thin films. The optimized etching conditions are: H_2 (30 mL/min), Ar (50 mL/min), working pressure (2 Pa), operating voltage

(90 V), and power (200 W).

3 Results and discussion

X-ray diffraction (XRD) was first used to determine the crystal structure and phase purity of the as-synthesized films. Figure 1(a) shows the XRD patterns of the CZTS films S1 and S2 fabricated with precursors S1 and S2, respectively. In both cases, three strong diffraction peaks at 28.86°, 47.74°, and 56.58° can be indexed well to the kesterite CZTS (JCPDS# 26-0575), indicating that both films could be kesterite CZTS. The peaks at 40.86° and 74.02° can be ascribed to the diffraction from the Mo substrate (JCPDS# 42-1120). No extra peaks are observed in the XRD patterns. Also, by comparing the XRD patterns of the films fabricated with precursors S1 and S2 with that of the Mo substrate, it can be seen that the film S1 has relatively higher diffraction intensities and smaller full width at half maximum (FWHM) for three strong peaks. According to the Scherrer equation, smaller FWHM corresponds to larger grain and better crystallinity. Therefore, it can be concluded that the CZTS film S1 was composed of larger grains.

Because the X-ray diffractions of binary and ternary chalcogenides (e.g., ZnS and Cu_2SnS_3) may overlap with that of the CZTS pattern, it is difficult to identify the CZTS simply by XRD patterns [25, 30, 31]. Raman spectroscopy was usually used to investigate the phase purity and composition of kesterite materials [32]. According to previous reports, the Raman shift of the CZTS will be mainly at 331–338 cm^{-1} with two additional peaks at 287 and 368 cm^{-1} [30, 32–37]. Figure 1(b) shows the typical Raman spectra of the CZTS films prepared in this work. Both spectra present a major peak located at 332 cm^{-1} with weak peaks at 287 and 368 cm^{-1}. No other peaks, including the ones from the binary or ternary chalcogenide such as Cu_2SnS_3, ZnS, $Cu_{2-x}S$, or SnS, were observed [33, 38]. Taking into account the XRD and Raman results together, it can be confirmed that the prepared CZTS films should be composed of a single-phase CZTS.

It was reported that CZTSSe TFSC usually demonstrated higher power conversion efficiency than CZTS TFSC because of better light absorption and thus larger short-circuit current density [2, 39, 40]. CZTSSe thin films can be obtained by selenizing CZTS thin films. Figure 1(c) presents typical XRD patterns of CZTSSe films S1 and S2. Comp-

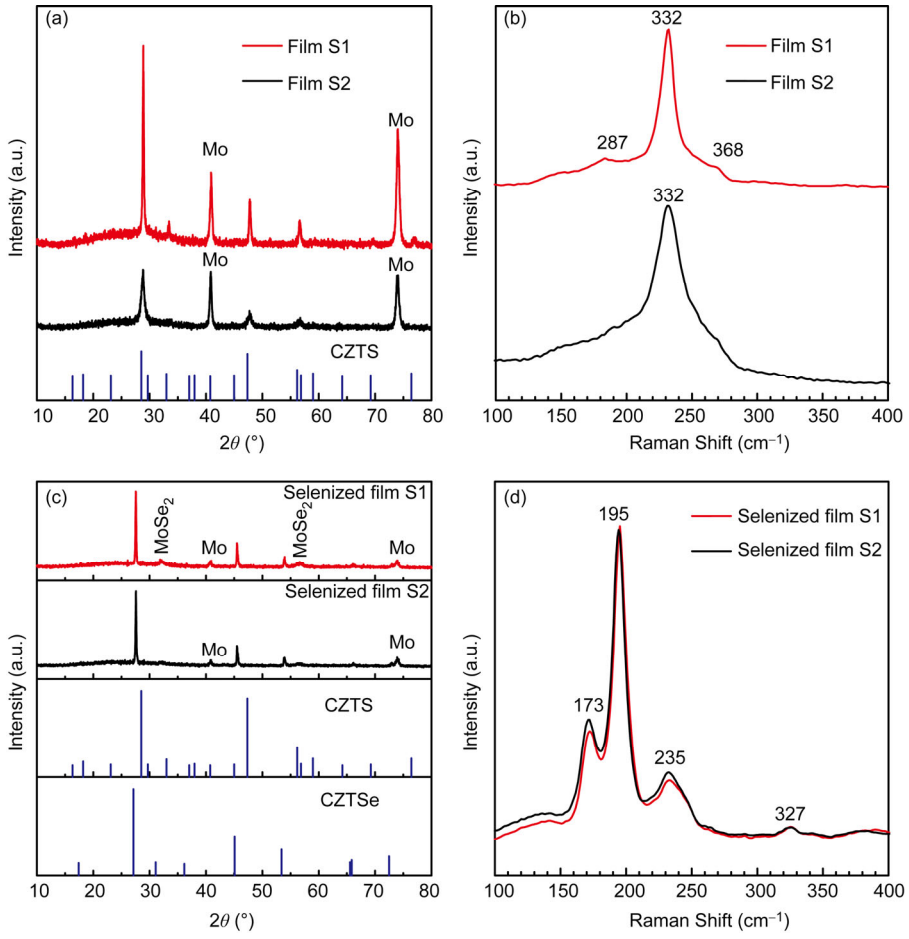

Figure 1 XRD profiles (a, c) and Raman spectra (b, d) of films prepared from different precursors S1 and S2. (a, b) CZTS films; (c, d) CZTSSe films.

ared with the standard XRD data of the CZTS (JCPDS# 26-0575) and CZTSe (JCPDS# 52-0868), the positions of the diffraction peaks for both selenized films located between the corresponding diffraction positions for pure CZTS and CZTSe, as reported in the literature [41]. As we know, the S/Se ratio could affect the diffraction peak position [42]. In both patterns, there are no other peaks observed except for the diffraction peaks from Mo substrate and $MoSe_2$ generated during selenization [7]. XRD data reveal that the CZTS films should be converted to CZTSSe films after selenization. Also, in reference to the diffraction peaks of Mo substrate, we can find that the intensities of diffraction peaks for CZTSSe films were significantly enhanced comparing with CZTS films, which means that further crystallization was achieved in selenization process. The Raman spectra were also recorded on both CZTSSe films. As shown in Figure 1(d), a strong peak at 195 cm^{-1} with two additional peaks at 173 and 235 cm^{-1} are clearly distinguished, which are typical Raman vibration features from CZTSSe [7]. The Raman signal of 327 cm^{-1} is consistent with the results previously reported [42]. No extra peaks were observed in Raman spectra, indicating that the prepared films after selenization consisted of a single-phase CZTSSe.

The morphologies of CZTSSe thin films were further investigated by SEM. Figure 2 shows typical top-view and cross-sectional view SEM images of the CZTSSe films prepared from two kinds of precursors. The low-magnification SEM images of the two films were shown in Figures S1 and S2 (Supporting Information online). It can clearly be seen that the CZTSSe film prepared with precursor S1 is composed of large and compact crystals in a size of submicrometers to micrometers (Figure 2(a)). The film is relatively flat and void-free. The thickness of the film is about 1.2 μm. As shown in the cross-sectional view SEM image in Figure 2(b), most of the CZTSSe crystals grew through the film and no small particle layer was found in the film. There are also no other layers such as carbon-rich small grain layer like that previously reported between CZTSSe absorber layer and the Mo/$MoSe_2$ substrate [25]. These features are believed to favor the carrier transport and lessen the carrier recombination center, and thus benefit the enhancement of power conversion efficiency. Energy dispersive X-ray spectroscopy (EDS) was used to analyze the composition of the film. EDS spectrum in Figure 2(c) shows that the film is composed only of element Cu, Zn, Sn, S, and Se. Corroborating the film is the CZTSSe. The quantitative analysis reveals that the atom ratio of Cu/(Zn+Sn) is 0.80 and Zn/Sn is 1.16. This result indicates that the prepared film is Cu-poor and Zn-rich CZTSSe, which is preferable for high-efficient devices [7]. On the contrary, CZTSSe film prepared with precursor S2 obviously comprises two different layers (Figure 2(d, e)): a top layer with larger crystal grain in micrometers and a bottom layer with small particles in tens of nanometers. The large discrete crystal grains do not connect into a continuous layer. An appreciable amount

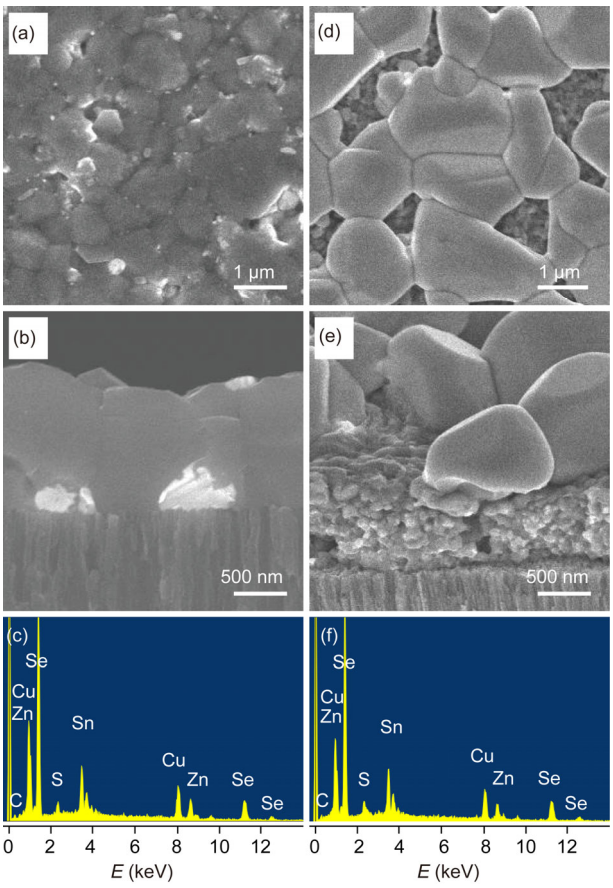

Figure 2 Top-view (a, d), cross-sectional view (b, e) SEM images, and EDS spectrum (c, f) of the CZTSSe film. (a–c) Prepared from the precursor S1; (d–f) prepared from the precursor S2.

of voids remain in the top layer. The small particle layer in over 500 nm thick exists between the CZTSSe layer and the substrate. The EDS spectrum (Figure 2(f)) recorded on the large crystal grain in film S2 also verifies the composition of CZTSSe. The quantitative analysis gives Cu/(Zn+Sn) of 0.81 and Zn/Sn of 1.08. Although the results in XRD, Raman, and EDS analyses show that the top layer of the film S2 is also preferable Cu-poor and Zn-rich CZTSSe, the discontinuous and layered structure of the film will severely degrade the device performance [7]. Comparing the preparation condition for two films, the only difference is the preparation atmosphere of the metal organic precursors (argon for film S1 and air for film S2). It can therefore be assumed that the existence of oxygen during the preparation of precursors could significantly influence the morphologies of final CZTSSe films in view of the fact that Cu^+ is easy to be oxidized. To further investigate this effect, another metal organic precursor S3 was prepared in the same procedure as precursor S1 except for using oxygen flow instead of argon flow. Figure 3(a, b) presents typical SEM images of the CZTSSe film S3. It can be seen that the film is mainly composed of small particles. The amount of large crystal grain becomes even much less than that in film S2. Although

the film S3 shows the similar features in XRD and Raman data (Figure 3(c, d)), which indicates that it has similar crystal structure and composition to other two films, this morphology is not suitable for absorber layer. The result suggests that the existence of oxygen during the preparation of the precursor will have undesirable influence on the morphology of the final film and should be precluded.

It is known that carbon residue in the CZTSSe absorber layer will appreciably deteriorate the quality of the p-n junction and thus degrade the device performance. It was found the amount of carbon residue closely depended on the processing parameters during the film preparation such as annealing temperature, selenization temperature, and temperature ramping rate. By optimizing all these processing parameters, we were able to minimize the formation of carbon residue and prepared all samples with these optimized parameters in this study. No obvious carbon-rich layer can be found in the prepared CZTSSe film, as shown in Figure 2(a, b). However, it is difficult to completely prevent the formation of carbon residues using non-hydrazine organic solvents to prepare absorber thin films. Although EDS results in Figure 2(c) did not show obvious signal of carbon, it does not mean that there is no trace amount of carbon residue on the surface of film. Raman spectroscopy is sensitive to detect the trace carbon on the surface. As shown in Figure 4, the Raman spectra of the as-prepared CZTSSe film S1 does show obvious Raman vibration signal of carbon at high wavenumbers (1000–1700 cm^{-1}) [43]. As we know, RIE is a dry etching technique widely used in the fabrication of electronic devices. During the RIE processing, Ar^+ ions are accelerated in the electric field, and bomb the sample surface. The generated particles react with the reactive radicles suffusing the chamber, and were then etched away [43–46]. To eliminate the trace amount of carbon residue,

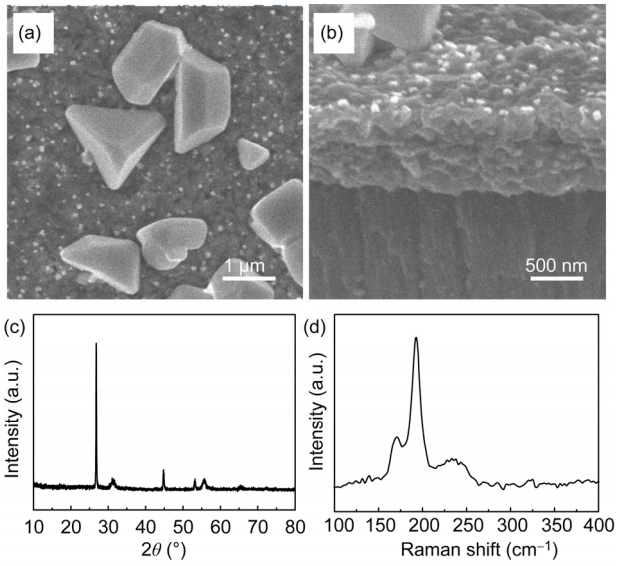

Figure 3 Top-view (a), cross-sectional-view (b) SEM images, XRD pattern (c), and Raman spectrum (d) of the CZTSSe film fabricated from precursor S3, which was synthesized under an oxygen flow.

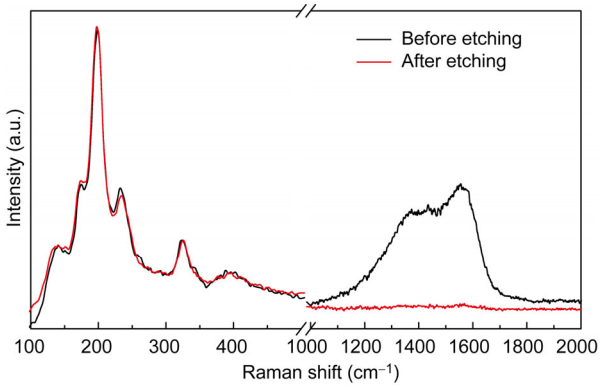

Figure 4 Raman spectra of the CZTSSe film S1 before and after RIE etching for 5 min.

RIE processing was carried out in this study to demonstrate its capability for removing carbon. Figure 4 shows the Raman spectra of the CZTSSe thin film before and after RIE etching. It can be clearly seen that the Raman signal peaks of carbon (1000–1700 cm^{-1}) totally disappear after 5 min RIE etching. At the same time, the characteristic Raman features of the CZTSSe at low wavenumbers (100–450 cm^{-1}) do not change before and after etching, indicating that the kesterite CZTSSe film was not affected and no other compounds or phases were generated after RIE processing. This result demonstrates that RIE technique can be safely used to remove carbon residue in the CZTSSe film after optimizing the etching conditions.

4 Conclusions

In conclusion, a non-hydrazine solution-based method has been developed to fabricate highly crystallized and carbon-free kesterite CZTSSe thin films by using soluble metal organic precursor to generate CZTS film followed converting it to CZTSSe film via selenization. Interestingly, it was found that the preparation atmosphere of metal-organic precursors significantly influence the morphology and crystallinity of the absorber film. When the precursor was synthesized in argon, a kesterite CZTSSe film composed of compact larger crystal grains was obtained, which are preferable for the absorber layer in the CZTSSe thin film solar cells. Although the precursor was synthesized in air, the film consisted of discrete larger crystal grain layer on top and small particle layer on bottom. Also, by optimizing the processing parameters, we were able to minimize the formation of harmful carbon residue in the CZTSSe film. Lastly, a viable RIE processing with optimized etching conditions was successfully developed to eliminate trace carbon residue on the surface of the CZTSSe film. Further work to fabricate the CZTSSe thin film solar cells is in progress.

This work was financially supported by the National Natural Science Foundation of China (21173237, 91127044, 21121063), the National Basic

Research Program of China (2011CB808700, 2012CB932900), and the Chinese Academy of Sciences.

1 Shah A, Torres P, Tscharner R, Wyrsch N, Keppner H. Photovoltaic technology: the case for thin-film solar cells. *Science*, 1999, 285: 692–698
2 Todorov TK, Tang J, Bag S, Gunawan O, Gokmen T, Zhu Y, Mitzi DB. Beyond 11% efficiency: characteristics of state-of-the-art $Cu_2ZnSn(S,Se)_4$ solar cells. *Adv Energy Mater*, 2013, 3: 34–38
3 Bag S, Gunawan O, Gokmen T, Zhu Y, Todorov TK, Mitzi DB. Low band gap liquid-processed CZTSe solar cell with 10.1% efficiency. *Energy Environ Sci*, 2012, 5: 7060–7065
4 Cao AM, Hu JS, Wan LJ. Morphology control and shape evolution in 3d hierarchical superstructures. *Sci China Chem*, 2012, 55: 2249–2256
5 Green MA, Emery K, Hishikawa Y, Warta W, Dunlop ED. Solar cell efficiency tables (version 42). *Prog Photovolt: Res Appl*, 2013, 21: 827–837
6 Jackson P, Hariskos D, Wuerz R, Wischmann W, Powalla M. Compositional investigation of potassium doped $Cu(In,Ga)Se_2$ solar cells with efficiencies up to 20.8%. *Phys Status Solidi RRL*, 2014, 8: 219–222
7 Mitzi DB, Gunawan O, Todorov TK, Wang K, Guha S. The path towards a high-performance solution-processed kesterite solar cell. *Sol Energy Mat Sol C*, 2011, 95: 1421–1436
8 Katagiri H, Jimbo K, Maw WS, Oishi K, Yamazaki M, Araki H, Takeuchi A. Development of CZTS-based thin film solar cells. *Thin Solid Films*, 2009, 517: 2455–2460
9 Ramasamy K, Malik MA, O'Brien P. Routes to copper zinc tin sulfide Cu_2ZnSnS_4 a potential material for solar cells. *Chem Commun*, 2012, 48: 5703–5714
10 Todorov TK, Reuter KB, Mitzi DB. High-efficiency solar cell with earth-abundant liquid-processed absorber. *Adv Mater*, 2010, 22: E156–E159
11 Guo Q, Ford GM, Yang WC, Walker BC, Stach EA, Hillhouse HW, Agrawal R. Fabrication of 7.2% efficient CZTSSe solar cells using CZTS nanocrystals. *J Am Chem Soc*, 2010, 132: 17384–17386
12 Steinhagen C, Panthani MG, Akhavan V, Goodfellow B, Koo B, Korgel BA. Synthesis of Cu_2ZnSnS_4 nanocrystals for use in low-cost photovoltaics. *J Am Chem Soc*, 2009, 131: 12554–12555
13 Walsh A, Chen S, Wei SH, Gong XG. Kesterite thin-film solar cells: advances in materials modelling of Cu_2ZnSnS_4. *Adv Energy Mater*, 2012, 2: 400–409
14 Woo K, Kim Y, Moon J. A non-toxic, solution-processed, earth abundant absorbing layer for thin-film solar cells. *Energy Environ Sci*, 2012, 5: 5340–5345
15 Shin B, Gunawan O, Zhu Y, Bojarczuk NA, Chey SJ, Guha S. Thin film solar cell with 8.4% power conversion efficiency using an earth-abundant Cu_2ZnSnS_4 absorber. *Prog Photovolt: Res Appl*, 2013, 21: 72–76
16 Katagiri H, Sasaguchi N, Hando S, Hoshino S, Ohashi J, Yokota T. Preparation and evaluation of Cu_2ZnSnS_4 thin films by sulfurization of E-B evaporated precursors. *Sol Energy Mat Sol C*, 1997, 49: 407–414
17 Cho JW, Ismail A, Park SJ, Kim W, Yoon S, Min BK. Synthesis of Cu_2ZnSnS_4 thin films by a precursor solution paste for thin film solar cell applications. *ACS Appl Mater Interf*, 2013, 5: 4162–4165
18 Fairbrother A, García-Hemme E, Izquierdo-Roca V, Fontané X, Pulgarín-Agudelo FA, Vigil-Galán O, Pérez-Rodríguez A, Saucedo E. Development of a selective chemical etch to improve the conversion efficiency of Zn-rich Cu_2ZnSnS_4 solar cells. *J Am Chem Soc*, 2012, 134: 8018–8021
19 Repins I, Beall C, Vora N, DeHart C, Kuciauskas D, Dippo P, To B, Mann J, Hsu WC, Goodrich A, Noufi R. Co-evaporated $Cu_2ZnSnSe_4$ films and devices. *Sol Energy Mat Sol C*, 2012, 101: 154–159
20 Chawla V, Clemens B. Effect of composition on high efficiency CZTSSe devices fabricated using co-sputtering of compound targets. In: 38*th IEEE Photovoltaic Specialists Conference.* Austin, 2012
21 Ahmed S, Reuter KB, Gunawan O, Guo L, Romankiw LT, Deligianni H. A high efficiency electrodeposited Cu_2ZnSnS_4 solar cell. *Adv Energy Mater*, 2012, 2: 253–259
22 Ki W, Hillhouse HW. Earth-abundant element photovoltaics directly from soluble precursors with high yield using a non-toxic solvent. *Adv Energy Mater*, 2011, 1: 732–735
23 Guo QJ, Ford GM, Yang WC, Hages CJ, Hillhouse HW, Agrawal R. Enhancing the performance of CZTSSe solar cells with Ge alloying. *Sol Energy Mat Sol C*, 2012, 105: 132–136
24 Yang W, Duan HS, Bob B, Zhou H, Lei B, Chung CH, Li SH, Hou WW, Yang Y. Novel solution processing of high-efficiency earth-abundant $Cu_2ZnSn(S,Se)_4$ solar cells. *Adv Mater*, 2012, 24: 6323–6329
25 Cao YY, Denny MS, Caspar JV, Farneth WE, Guo QJ, Ionkin AS, Johnson LK, Lu MJ, Malajovich I, Radu D, Rosenfeld HD, Choudhury KR, Wu W. High-efficiency solution-processed $Cu_2ZnSn(S,Se)_4$ thin-film solar cells prepared from binary and ternary nanoparticles. *J Am Chem Soc*, 2012, 134: 15644–15647
26 Guo Q, Hillhouse HW, Agrawal R. Synthesis of Cu_2ZnSnS_4 nanocrystal ink and its use for solar cells. *J Am Chem Soc*, 2009, 131: 11672–11673
27 Wang G, Zhao W, Tian Q, Huang L, Pan D, Cui Y, Gao S. Fabrication of $Cu_2ZnSn(S,Se)_4$ photovoltaic device by a low-toxic ethanol solution process. *ACS Appl Mater Interf*, 2013, 5: 10042–10047
28 Hsu CJ, Duan HS, Yang W, Zhou H, Yang Y. Benign solutions and innovative sequential annealing processes for high performance $Cu_2ZnSn(S,Se)_4$ photovoltaics. *Adv Energy Mater*, 2014, 4, 1301287
29 Wang Y, Gong H. Low temperature synthesized quaternary chalcogenide Cu_2ZnSnS_4 from nano-crystallite binary sulfides. *J Electrochem Soc*, 2011, 158: H800–H803
30 Schorr S, Weber A, Honkimaki V, Schock HW. *In-situ* investigation of the kesterite formation from binary and ternary sulphides. *Thin Solid Films*, 2009, 517: 2461–2464
31 Weber A, Mainz R, Unold T, Schorr S, Schock HW. *In-situ* XRD on formation reactions of Cu_2ZnSnS_4 thin films. *Phys Status Solidi C*, 2009, 6: 1245–1248
32 Cheng AJ, Manno M, Khare A, Leighton C, Campbell SA, Aydil ES. Imaging and phase identification of Cu_2ZnSnS_4 thin films using confocal raman spectroscopy. *J Vac Sci Technol A*, 2011, 29: 051203
33 Fernandes PA, Salome PMP, da Cunha AF. Growth and raman scattering characterization of Cu_2ZnSnS_4 thin films. *Thin Solid Films*, 2009, 517: 2519–2523
34 Sarswat PK, Free ML, Tiwari A. Temperature-dependent study of the raman a mode of Cu_2ZnSnS_4 thin films. *Phys Status Solidi B*, 2011, 248: 2170–2174
35 Mitzi DB, Todorov TK, Gunawan O, Yuan M, Cao Q, Liu W, Reuter KB, Kuwahara M, Misumi K, Kellock AJ, Chey SJ, de Monsabert TG, Prabhakar A, Deline V, Fogel KE. Torwards marketable efficiency solution-processed kesterite and chalcopyrite photovoltaic devices. In: 35*th IEEE Photovoltaic Specialists Conference*. Honolulu, 2010
36 Altosaar M, Raudoja J, Timmo K, Danilson M, Grossberg M, Krustok J, Mellikov E. $Cu_2Zn_{1-x}Cd_xSn(Se_{1-y}S_y)_4$ solid solutions as absorber materials for solar cells. *Phys Status Solidi A*, 2008, 205: 167–170
37 Himmrich M, Haeuseler H. Far infrared studies on stannite and wurtzstannite type compounds. *Spectrochim Acta A*, 1991, 47: 933–942
38 Fernandes PA, Salome PMP, da Cunha AF. A study of ternary Cu_2SnS_3 and Cu_3SnS_4 thin films prepared by sulfurizing stacked metal precursors. *J Phys D-Appl Phys*, 2010, 43: 215403
39 Wang K, Gunawan O, Todorov T, Shin B, Chey SJ, Bojarczuk NA, Mitzi D, Guha S. Thermally evaporated Cu_2ZnSnS_4 solar cells. *Appl Phys Lett*, 2010, 97: 143508
40 Barkhouse DAR, Gunawan O, Gokmen T, Todorov TK, Mitzi DB. Device characteristics of a 10.1% hydrazine-processed Cu_2ZnSn

$(Se,S)_4$ solar cell. *Prog Photovolt: Res Appl*, 2012, 20: 6–11
41 Yin X, Tang C, Sun L, Shen Z, Gong H. Study on phase formation mechanism of non- and near-stoichiometric CZTSSe film prepared by selenization of Cu-Sn-Zn-S precursors. *Chem Mater*, 2014, 26: 2005–2014
42 Zhao Y, Han X, Li W, Liu L, Tanaka T. Synthesis of the $Cu_2ZnSn(S,Se)_4$ alloys with tunable phase structure and composition via a novel non-toxic solution method. *Rsc Adv*, 2013, 3: 26160–26165
43 Lee HJ, Kwon BS, Park YR, Ahn JH, Kim JS, Lee NE, Shon JW. Inductively coupled plasma etching of chemical-vapor-deposited amorphous carbon in N_2/H_2/Ar chemistries. *J Korean Phys Soc*, 2010, 56: 1441–1445
44 Urakawa T, Torigoe R, Matsuzaki H, Yamashita D, Uchida G, Koga K, Shiratani M, Setsuhara Y, Takeda K, Sekine M, Hori M. H_2/N_2 plasma etching rate of carbon films deposited by H-assisted plasma chemical vapor deposition. *Jpn J Appl Phys*, 2013: *5*201AB01
45 Braginsky OV, Kovalev AS, Lopaev DV, Malykhin EM, Rakhimova TV, Rakhimov AT, Vasilieva AN, Zyryanov SM, Koshelev KN, Krivtsun VM, van Kaampen M, Glushkov D. Removal of amorphous C and Sn on Mo:Si multilayer mirror surface in hydrogen plasma and afterglow. *J Appl Phys*, 2012, 111: 093304
46 Hansen TAR, Weber JW, Colsters PGJ, Mestrom D, van de Sanden MCM, Engeln R. Synergistic etch rates during low-energetic plasma etching of hydrogenated amorphous carbon. *J Appl Phys*, 2012, 112: 013302